

Micromorphology and adhesive properties of sulfonated polyurethane/polyacrylate emulsions prepared by surfactant-free polymerization

Guoyan Ma¹ · Yiding Shen¹ · Ruimin Gao² · Xiaorong Wang³

Received: 14 October 2016 / Accepted: 6 February 2017 / Published online: 9 February 2017
© Springer Science+Business Media Dordrecht 2017

Abstract Novel eco-friendly sulfonated polyurethane/polyacrylate (SPUA) emulsions were synthesized by surfactant-free emulsion polymerization method using PU as seeds. The sodium sulfonate modified polyester polyol (SDNP) was used as internal emulsifier to make the PU emulsion disperse in deionized water. Effects of the SDNP content on the properties of the emulsions and membranes were studied. Dynamic light scattering (DLS) result showed that the average particle sizes of SPUA emulsions decreased first from 124.1 nm to 102 nm when the SDNP content was lower than 40 wt% and then increased to 138 nm. Transmission electron microscopy (TEM) morphology showed that the particle sizes were all spherical and an apparent core-shell structure was observed. Fourier transform infrared spectroscopy (FT-IR) result ascertains that SPUA was successfully prepared. X-ray photoelectron spectroscopy (XPS) analysis demonstrates that the carbon, oxygen, nitrogen, sulfur, and sodium peaks were all revealed and the polyurethane component was rich in the upper surface. Thermo gravimetric analysis (TGA) of the membranes showed that the thermal stability of the SPUA membranes was enhanced by increasing the SDNP content. Scanning electron micrograph (SEM) results demonstrates

that the coexistence of a dual phase. The SPUA could be used as adhesives in footwear industry, and the T-peel strength of the SPUA membranes increased from 5.98 N/mm to 12.06 N/mm when the SDNP content was up to 40 wt%. The wettability of SPUA emulsions on the rubber surface results showed that the emulsions could wet the rubber surface well.

Keywords Sulfonated polyurethane/polyacrylate · Properties and characterization · Micromorphology · Wettability

Introduction

Due to the increasing concern about environmental pollution, health and safety risks, regulatory, waterborne polyurethane emulsions have been gradually replaced the solvent-borne polyurethanes [1]. Amount of organic solvents were used in prepared the conventional solvent-borne polyurethane products, and the solvents were very harmful to the environment. The solvent of waterborne polyurethane (WPU) was water, and it did no harm to the environment and health of human. Waterborne polyurethane (WPU) polymer films were of great interest for applications in coatings, adhesives, sealants and the textile industry [2–4].

Generally, pristine polyurethane prepolymers are not hydrophile and not soluble in water. Therefore, they must be soluble in water by incorporating hydrophilic monomers or monomers containing ionic groups such as quaternary ammonium or carboxylate into the polymer structure [5–7]. These monomers acted as an internal emulsifier. The dimethylol propionic acid (DMPA) with pendant carboxyl group is one of the most commonly used hydrophilic monomers, which can be introduced into the PU chains by reacting with NCO groups of its two OH groups. The prepared PU dispersions with DMPA content can be dispersed in water after neutralized by tertiary amines [8, 9]. But with the addition of tertiary

✉ Guoyan Ma
522507100@qq.com; guoyanma@163.com

¹ Present address: Key laboratory of Auxiliary Chemistry & Technology for Chemical Industry, Ministry of Education, Shaanxi University of Science & Technology, Weiyang District, Xi'an, Shaanxi Province 710021, China
² Research Institute of Shaanxi Yanchang Petroleum (Group) Co., Ltd., Xi'an, Shaanxi Province 710015, China
³ College of Chemistry and Chemical Engineering, Xianyang Normal University, Shaanxi province, Xianyang 712000, China

amines, the preparation process may be more complex. The tertiary amines has a strong amine taste, and it also could do some harm to the environment and health of human.

As the drawbacks of the DMPA, in this study, we have attempted to introduce sodium sulfonate modified polyester polyol as a potential substitute for DMPA into the PU chains. The monomers containing sodium sulfonate group can also be used to prepare anionic PU emulsions. The sodium sulfonate modified polyester polyol possessed a side chain with sodium sulfonate groups, designated as SDNP. The SDNP could be introduced into the PU backbone due to the reactivity of its two OH groups with reaction of NCO groups. Compared with DMPA based PU emulsions, sulfonated polyurethane emulsions show an excellent hydrolytic stability over a wide range of pH values [10]. SDNP was a polydiol sodium with a strong acid and a strong base structure, so the ionization degree was higher. It could form a more stable double electron layer structure, which was helpful to enhance the solid content and stability of the PU.

Owing to the presence of hydrophilic groups in the PU backbone, the PU membranes showed some weak water-resistance and poor membrane performance [11]. One measurement to improve the performance is to combine PU with other polymers, such as polyacrylate (PA). PA emulsions possess good mechanical properties and outstanding climate and water resistance performances. The composite emulsion of polyurethane/polyacrylate combines the excellent properties of PU emulsion and PA polymers, which could greatly improve the properties of the PU membranes. The acrylate monomers are incorporated by surfactant-free emulsion polymerization and the PU emulsion could use as seeds since it built up with a similar amphiphilic molecular structure like traditional surfactants. The PU dispersion acted as not only macromonomers but also macromolecular emulsifier [12, 13]. Pentaerythritol triacrylate (PETA), acrylate monomers with one hydroxyl and three vinyl groups, could terminate the PU chains with the double bond and also react with other acrylate monomers with the three vinyl groups. It performed as the bridge of the copolymerization reactions to further enhance the properties of the membranes. Both polymers are present in a single latex particle and form core-shell structure.

The main approach of this study was to prepare the efficient aqueous PU emulsions with sodium sulfonate modified polyester polyol. The acrylate monomers were used to replace the organic solvent in the preparation process of the PU prepolymer. PU was used as seeds in the soap-free emulsion polymerization. The initiator was added to initiate the free-radical polymerization of acrylate monomers to obtain the eco-friendly sulfonated polyurethane/polyacrylate (SPUA) emulsions. In this article, SPUA composite emulsions with different SDNP were prepared. Dynamic light scattering (DLS), Transmission electron microscopy (TEM), Fourier transform infrared spectroscopy (FTIR), X-ray photoelectron spectroscopy (XPS), electronic tensile machine, Thermal

gravimetric analysis (TGA), Differential scanning calorimetry (DSC), Dynamic mechanical thermal analyses (DMA) and Scanning electron microscope (SEM) were employed to investigate the structures and properties of the composite emulsions and their membranes. The obtained SPUA could be used as adhesives in the footwear industry since the smaller particles could penetrate into a substrate easily. The effect of SDNP on the T-peel strength, surface tension and contact angle were also investigated to characterize the adhesive property.

Experimental

Materials

Isophorone diisocyanate (IPDI), 1,4-Butylene glycol (BDO) were supplied by Sinopharm Chemical Reagent Co., Ltd.; sodium sulfonate modified polyester polyol (SDNP, $M_n = 2000$) was purchased from Beijing Baiyuan Chemical Co., Ltd.; Dibutyltin dilaurate (DBTDL), Tetrahydrofuran (THF), Methyl methacrylate (MMA), 2-Hydroxyethyl acrylate (HEA), potassium persulfate (KPS), Butyl acrylate (BA) produced by Tianjin Hongyan Chemical Reagent Co., Ltd.; Pentaerythritol triacrylate (PETA) was supplied by Jinjin Chemical Co., Ltd., respectively. All raw materials are laboratory grade chemicals and were used as received without further purification. SDNP were dried in vacuum before use.

Preparation of SPUA composite emulsions and membranes

The synthesis of the SPUA composite emulsions was carried out in a 500 mL four-necked glass reactor equipped with a mechanical stirrer, a thermometer, a nitrogen inlet and a condenser with a CaCl_2 drying tube. The IPDI, SDNP and catalyst DBTDL were added into the reactor and the reaction was carried out at 80 °C for 2 h to obtain an NCO-terminal hydrophilic PU prepolymer. BDO and a mixture of MMA and BA (5 wt% of the total MMA and BA amount) were added into the system and reacted for 1.5 h. The addition of acrylic monomers could reduce the viscosity of PU prepolymer. The PETA was added into the system at 75 °C, and the double bond-ended PU prepolymer was obtained after reacted for 1.5 h. A calculated amount of deionized water was added to the mixture with vigorous stirring, and the SPU dispersions with a solid content of 30 wt% were obtained.

The core-shell SPUA composite emulsions were prepared by soap-free emulsion polymerization with the above-synthesized PU dispersion as seed particles. The PU dispersion acts not only as macro monomers but also as macromolecular emulsifier. The mixture monomers of MMA, BA (95 wt% of the total MMA and BA amount), and HEA were added dropwise into the PU dispersion at 80 °C in the radical polymerization stage. The

polymerization was carried out with KPS as initiator. The KPS initiator solution was subsequently added to the reactor to initiate the radical copolymerization of the vinyl monomers. When KPS was added into the dispersion, the double bond-end capped polyurethane and the acrylic monomers swollen in PU dispersion were initiated. The KPS was dropped into the reactor at 80 °C within 2 h, and the reaction was allowed to keep at 80 °C for additional 1 h. After completing copolymerization, the SPUA emulsions with different SDNP were prepared. The synthetic route is shown in Fig. 1. The sample designation and composition was shown in Table 1.

Homogeneous membranes for the tests were prepared by casting the emulsions onto a flat Teflon disk and drying under ambient conditions for 2 days and then at 60 °C for 24 h. After demoulding, the 1 mm thick membranes were obtained. The membranes were stored in desiccators to avoid moisture.

Characterization

The mean particle size and the particle size distribution of the SPUA emulsions were measured in a Malvern instruments (Malvern Zetasizer Nano ZS) by Dynamic Light Scattering

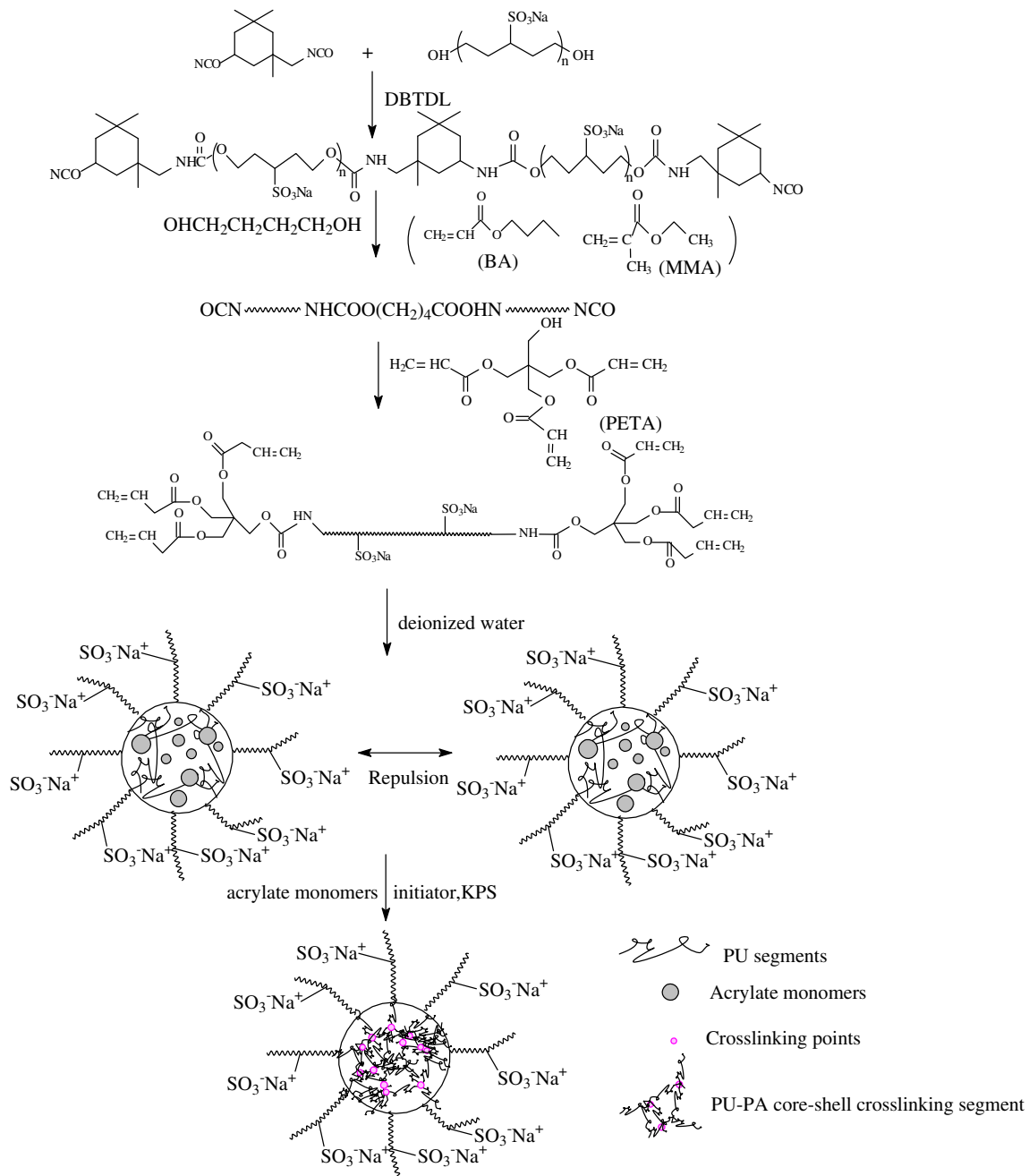


Fig. 1 Preparation process of the SPUA emulsions

Table 1 Sample Designation, Composition of SPUA Emulsions

Sample Designation	IPDI	SDNP	PETA	BDO	MMA*	BA*	HEA*	Acrylic content/(wt%)
SPUA1	23	30.5	0.8	1.75	56.6	28.5	15	30
SPUA2	26.6	35.5	0.8	1.75	56.6	28.5	15	30
SPUA3	30.4	40.5	0.8	1.75	56.6	28.5	15	30
SPUA4	34.1	45.5	0.8	1.75	56.6	28.5	15	30
SPUA5	37.9	50.5	0.8	1.75	56.6	28.5	15	30

*The mass ratio of MMA/BA/HEA is 3.77/1.9/1

(DLS) method. The SPUA emulsions were diluted with deionized water to 0.5 wt% before the measurement. The temperature of the cell was kept at around 25 °C and the equilibrium time was 120 s. The mean particle size and the particle size distribution were characterized automatically by the computer connected to the machine.

The morphology of the SPUA emulsions was characterized by the transmission electron microscope (TEM) observations. The experiments were carried out on an H-600 electron microscope (Hitachi Co., Japan). The SPUA emulsions prepared were diluted with deionized water to about 0.5 wt%. The samples were prepared by depositing a drop of well diluted blend suspension onto a 200-mesh copper grid and allowing it to set for 10 min. After drying, the samples were stained with phosphotungstic acid for another 10 min.

The chemical structure of SPUA membrane was analysed by using Attenuated total reflection fourier transform infrared (ATR-FTIR) method. The measurements were performed on a model V70 infrared spectrophotometer at ambient temperature with a wave number resolution of 4 cm⁻¹. The ATR-FTIR spectrum of the dried sample membrane was obtained by using the attenuated total reflectance mode.

The surfaces of the SPUA membranes were analyzed with X-ray photoelectron spectroscopy (XPS). The XPS spectra were obtained by Axis Ultra Kratos using monochromatic Al K α radiation (150 W, 15 kV, 1486.6 eV). The dry emulsion membrane was prepared on the monocrystalline silicon wafer by removing all the water and moisture under vacuum condition at room temperature. The vacuum in the spectrometer was 10⁻⁹ Torr. The unique set of binding energies of each element was used to identify and determine the concentration of the elements on the surface.

Stress-strain curves and Young's modulus of membranes were measured on a universal testing machine (CMT6503 mode) according to the Chinese standard ISO527-3:1995 with a crosshead speed of 100 mm/min at room temperature. Rectangular-shaped specimens with dimensions of 10.0 mm × 25.0 mm × 1 mm were used for the measurement. The results were obtained for each sample and the values quoted were the calculated average of three measurements.

Thermal gravimetric (TG) experiments were performed in a Q500 thermogravimeter (TA Instruments Company, USA) to

measure the weight losses of SPUA membranes in the temperature range 30–500 °C with a heating rate of 10 °C/min under the nitrogen atmosphere. The samples were placed in platinum sample pans. Only one test was made for each sample.

The thermal behavior of the SPUA membranes were carried out on the Differential scanning calorimetry (DSC) Q200 differential scanning calorimeter (TA Instruments Company, USA). 10 ± 1 mg of the samples was placed in an aluminium pan under nitrogen atmosphere by using a heating rate of 10 °C/min (flow rate: 20 ml/min). The samples were subjected to the heating/cooling cycle between -100 and 200 °C under a nitrogen atmosphere (flow rate: 20 ml/min) [14].

Dynamic mechanical thermal analyses were performed using a dynamic mechanical analysis instrument (Q800, TA Instruments) in tension mode. Rectangular-shaped specimens with dimensions of 6.0 mm × 20.0 mm × 0.6 mm were used for the measurement. The specimens were measured at a frequency of 1 Hz and strain of 0.1% in the temperature range of -90 °C to 150 °C.

Scanning electron micrograph of the fractured sections of SPUA membrane was obtained by using SEM (model JSM-6700F) at 50 kV. The specimens were freshly broken in liquid nitrogen, fractured, and then the fractured sections were coated with gold using an Edwards S 150A sputter coater. The morphology of the fractured sections of the films was examined.

The T-peel strengths of the SPUA emulsions were studied by T-peel strength tests of leather/SPUA/rubber joints using rubber strips of dimensions 150 × 30 × 4 mm. The rubber surface was covered the 0.5 ml emulsions uniformly and then the rubber was put into the oven to dry for 1 h at 60 °C. After evaporation, a thick-solid adhesive film was formed. The strips were then bonded with a suitable leather surface. They were immediately placed under a pressure for 3 min, and then put them at ambient temperature for 24 h before test. The T-peel strength values of the leather/SPUA/rubber joints tests were performed in a TS2000-S universal test machine with a crosshead speed of 500 mm/min.

Contact angles of emulsion on the surface of the rubber were measured using a JC2000A contact angle goniometer at room temperature [15]. Samples were fixed onto cleaned glass substrates. The films were dried at room temperature. Six parallel measurements on different points were performed to calculate the mean static contact angle.

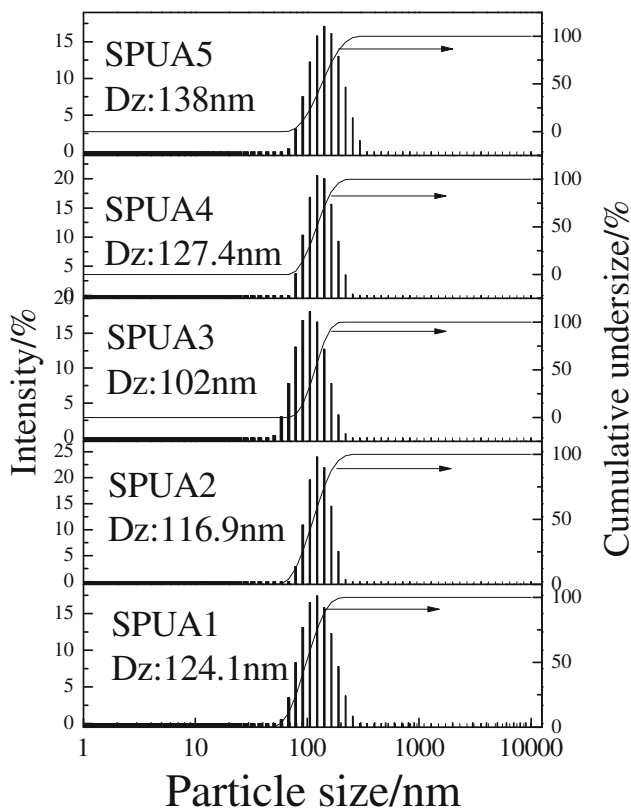


Fig. 2 Particle sizes of SPUA emulsions with different SDNP content

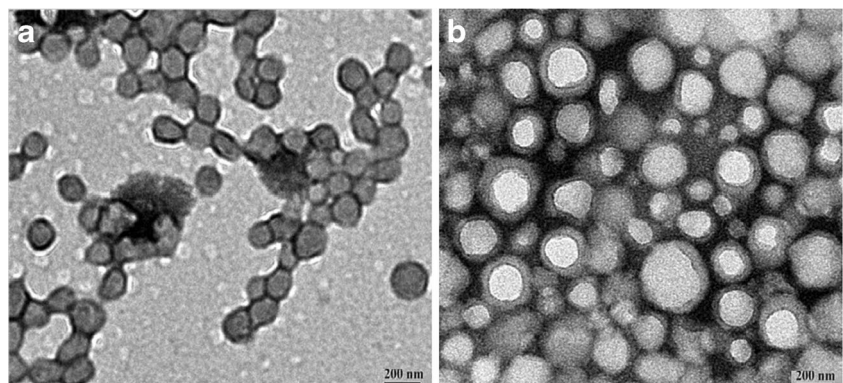
Surface tensions were measured by the ring method with XJZ-200 surface tensiometer (Chengde Jin Jian Testing Instrument) at 25 °C. Double distilled water ($\gamma = 72.1 \pm 0.01$ mN/m) and absolute alcohol ($\gamma = 22.3 \pm 0.01$ mN/m) were used to calibrate the instrument. The result was the mean of five replicates.

Results and discussion

Particle size and morphologies of the SPUA emulsions

The average particle sizes of SPUA emulsions with different SDNP contents were determined by a lazer-scattering

Fig. 3 TEM morphologies of SPU without PA (a) and SPUA3 (b)



technique, as shown in Fig. 2. The particle size decreased from 124.1 nm to 102 nm with increasing SDNP content, when the SDNP content was lower than 40 wt%. In the emulsions, SPUA contains $-\text{SO}_3^- \text{Na}^+$ groups. It means that with increasing of anionic center, the particle size first decreased [16]. The ionic centers are naturally hydrophilic and considerably located on the surfaces of the SPUA emulsion particles in the continuous aqueous media. In fact, each particle is surrounded by a thin layer of water due to the presence of hydrophilic $\text{SO}_3^- \text{Na}^+$ groups on the surface of the particles. With the augmentation of SDNP content, the hydrophobic groups are surrounded by hydrophilic $\text{SO}_3^- \text{Na}^+$ groups tightly. During the oil-water phase inversion, the prepolymers can easily be dispersed into smaller particles [17], which demonstrated as the decreasing particle size. With the further increment of the SDNP content, the particle size increased to 138 nm. The decreased particle size will produce an increase in the size of the double layer of the smaller ionomer particles, and SPUA emulsions (SPUA4 and SPUA5) containing more ionic groups possess stronger electrostatic interactions between particles, which results in the expanded network of the particles [18]. Therefore, the particle size increased with the content of SDNP is larger than 40 wt%.

The transmission electron microscopy morphology of the SPU without PA (a) and SPUA3 (b) were shown in Fig. 3 and they were amplified to eighty thousand times. It can be seen that the particle size were all more than 100 nm, and they were all spherical particles. As to SPU without PA, the size distribution was homogeneous. Compared with SPU without PA, with the addition of PA content, an apparent core-shell structure was observed due to the difference of electron penetrability to the core phase and the shell phase in SPUA3(b). The light region represents the core phase of polyacrylate, while the dark region represents the shell phase of polyurethane [11]. In the polymerization process, the hydrophilic PU segment tend to be close to the aqueous phase, and hydrophobic PA segment tend to be far away from the aqueous phase, which could form the stable SPUA emulsion with PU as shell and PA core.

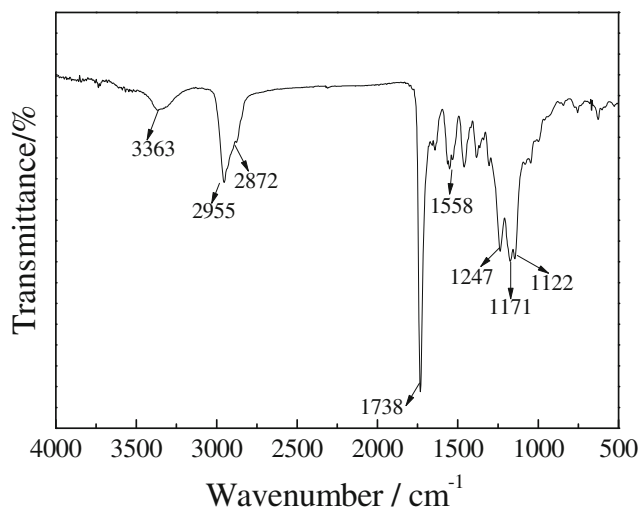


Fig. 4 The ATR-FTIR absorption peaks of SPUA3

ATR-FTIR spectroscopy analysis

Figure 4 demonstrates the typical ATR-FTIR spectrum of SPUA3. The absorption peak at 3363 cm^{-1} is due to the stretching of hydrogen bonding of N–H band. The bands at 1738 cm^{-1} are corresponding to the C = O of urethane and ester groups and the peaks at 1558 cm^{-1} are attributed to the bending vibration of N–H and stretching vibration of C–N. The peaks at 1122 cm^{-1} are due to the antisymmetric vibration of C–O–C. All these data confirm the formation of urethane group [13, 19]. There was no characteristic peak at 2200 cm^{-1} – 2300 cm^{-1} , which indicated that the group of N = C = O was completely reacted [12]. The asymmetric stretching of $-\text{CH}_3$ and $-\text{CH}_2-$ was located at 2955 cm^{-1} and 2872 cm^{-1} , respectively. The characteristics band of acrylic ester groups was observed at 1171 cm^{-1} which are attributed to the C–O stretching vibrations of acrylic ester groups. There was also no absorption peak at 1640 cm^{-1} , which demonstrated that the polyacrylate monomers took part in the emulsion polymerization completely [20]. The characteristics absorption peak at

Table 2 Surface chemical compositions for SPUA3 membranes

Element	Element/%		O1s Area/%	
	Experimental	Theoretical	C-(C = O)-O	$-\text{CH}_2\text{SO}_3\text{Na}$
C	59.72	68.93		
N	15.09	11.16		
O	23.01	18.46	83.15	16.85
S	1.65	1.23		
Na	0.53	0.22		

1247 cm^{-1} is corresponding to the asymmetric and symmetric stretching vibrations of sulfonate group. All these results of ATR-FTIR analysis ascertain that SPUA was successfully prepared.

Surface analysis of SPUA membranes

XPS analysis is widely used in the study of membranes for the surface chemical compositions [21]. The chemical elements of the interface of SPUA3 membrane was illustrated in Fig. 5a. It can be seen that the carbon, oxygen, nitrogen, sulfur, and sodium peaks were all revealed in Fig. 5a. The signal peaks at 285.32 eV were due to the C1s. The signal peaks at 399.81 eV were corresponding to the N1s. The signal peaks at 532.45 eV were attributed to the O1s. While the signal peaks in the XPS spectrum at 168.53 eV was assigned to sulfonate ion, the polar group of the sulfonate units [22]. The peaks at 978.61 eV are attributed to the Na elements in the sulfonate groups. The results demonstrate that the SDNP were successfully reacted in preparation of the SPUA emulsions. Table 2 demonstrates the compositions of C, N, O, S and Na elements on the surface of SPUA3 membranes. It can be seen that the content of N element in the experimental and theoretical measurements was almost the same, which could illustrate that the polyurethane component was rich in the upper surface. The results were in consistent with the TEM results.

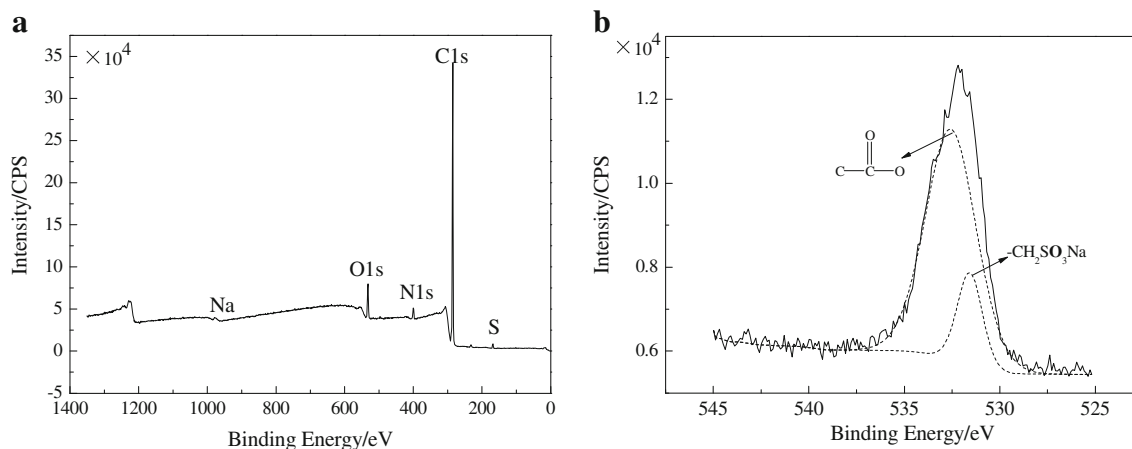


Fig. 5 Typical XPS spectrum of the membrane of SPUA3 interface (a); deconvolution of O1s XPS spectrum for the membrane of SPUA3 interface (b)

The O1s is located in a relatively simple chemical environment [23] in the SPUA chains. The peak deconvolution of O1s XPS spectrum for the membrane of SPUA3 interface was shown in Fig. 5b, and the computer automatic peak deconvolution results of the spectra were also shown in Table 2. The relative curves of O1s (Fig. 5b) were divided into two characteristic peaks, at 531.12eV, 533.38 eV, respectively. The signal peak at 531.12eV is corresponding to oxygen atom in the sodium sulfonate groups while the signal peak at 533.38eV is corresponding to oxygen atom in the urethane group or in ester group of the acrylate.

Mechanical properties of the membranes

The stress-strain curves of SPUA membranes with different SDNP content were studied and presented in Fig. 6. The tensile parameters obtained from Fig. 6 are presented in Table 3. Tensile strength and elongation at break were obtained from the stress-strain curves. It can be seen that with the increment of the SDNP content, the tensile strength and Young's modulus of the membranes increased significantly. The initial SPUA membrane had a tensile strength at 18.74 MPa, Young's modulus 12.76 MPa with 372% elongation at break when the SDNP content was 30%. The tensile strength has increased to 34.5 MPa, and Young's modulus increased to 21.72 MPa after the SDNP content increased to 50%. On the one hand, with the augment of sodium sulfonate groups, hydrogen bonding forces between the anion centers and urethane linkages were enhanced, and the coulombic forces between the ionic centers were also increased [17]. Hydrogen bonding forces and coulombic forces of the SPUA chains may be responsible for the increment of tensile strength and Young's modulus [24]. On the other hand, the sodium sulfonate groups were a sodium group with a strong acid and a strong base. The electrostatic interaction was very powerful, which caused

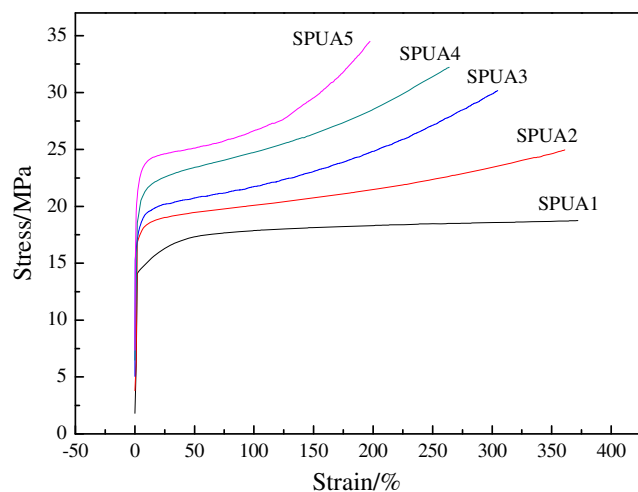


Fig. 6 Stress-strain curves of SPUA membranes with different SDNP content

Table 3 Results obtained from tensile test for SPUA membranes with different SDNP content

Sample	SPUA1	SPUA2	SPUA3	SPUA4	SPUA5
Stress at break/MPa	18.74	24.96	30.18	32.22	34.5
Young's modulus/MPa	12.76	16.48	18.53	20.41	21.72
Strain at break/%	372	361	304.6	264	197.5

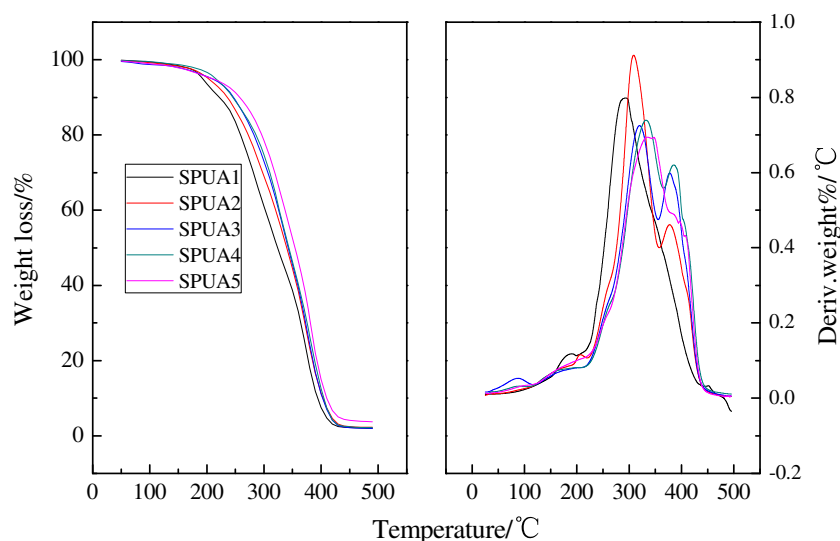
increased interchain interactions between the polymer chains. Therefore, with the increment of SDNP content, the SPUA membranes showed higher tensile strength, Young's modulus and lower elongation at break. Also, with the addition of PETA, the density of the crosslinking positions increases in the polymers. The crosslinking structure between the macromolecules prevents the slippage of the chains, which results in the increment of tensile strength and also the decrement of the elongation at break.

Thermo gravimetric analysis

The thermal stability was demonstrated by the widely used TGA measurements. Fig. 7 illustrates the thermal stability of the samples as a function of the SDNP content. The initial decomposition temperature (T_5), the half decomposition temperature (T_{50}), the final decomposition temperature (T_{90}), and the maximum weight-loss temperatures were summarized in Table 4. There is hardly any weight loss before 150 °C for all the samples. With the increment of the SDNP content, the decomposition temperature of the SPUA membranes increased gradually at the temperature ranged from 200 °C to 400 °C. It can be seen from Table 4, the T_{50} value increased from 317.17 °C to 349.73 °C. The thermal stability of the SPUA membranes was enhanced by increasing the SDNP content.

There were three different stages of degradation as shown in the differential thermogravimetric (DTG) curves, which was not perceptible in TG curves. The first stage at 183.48 °C to 208.71 °C was attributed to the urethane hard segment concentration [25, 26]. The temperature at 291.34 °C to 339.36 °C was corresponded to the degradation of the soft segment at the second stage. The increment of the SDNP content produces a gradually increase in the decomposition temperature. As the polarity of the sodium sulfonate group was stronger, the electrostatic interaction between the sodium sulfonate groups was strong [17]. The greater interchain interactions through coulombic forces and hydrogen bonding were then induced, which could enhance the thermal stability. The third stage at the temperature range 352.334 °C to 397.37 °C were due to the degradation of PA content. In general, the thermal stability of the SPUA polymers relied on the heat resistance of the groups in the macropolymer chains. With

Fig. 7 TGA curves for SPUA membranes with different SDNP content



the increment of the SDNP content, the thermal stability improved.

DSC analysis

The thermal response properties of the SPUA membranes were determined to by the differential scanning calorimetry (DSC) thermograms. The glass transition temperature (T_g) has been discussed in detail since it is directly reflected compatibility and interaction between the polymer chains. The typical DSC thermograms corresponding to the heating run of the SPUA3 and SPUA5 membranes are demonstrated in Fig. 8. It presented that the membranes showed two glass

transition temperatures according to the soft ($T_{g1,1'}$) and hard segments ($T_{g2,2'}$) and one melting peak (T_m) at 80–120 °C. With the increment of the SDNP content, the T_g value of the soft segment to decreased from -27.11 °C to -39.05 °C, and the T_g value of the hard segment decreased from 47.92 °C to 37.93 °C. Pérez-Limiñana et al. have showed that the increase in the ionic groups resulted in a decrease in the crystallinity [27]. Therefore, with the increment of the sulfonate content, the increased in the anion groups produces a decrease in the crystallinity, which will decrease the T_g value [27]. From Fig. 8, it also presented that the T_m decreased as the SDNP content increased. With the increment of the polar groups, the electrostatic repulsion between the polymer chains increases, then the perfection of the crystal became lower, which caused the T_m value decreased.

Table 4 TGA Data for SPUA membranes

Designation	TG/°C			DTG peaks/°C
	T_5	T_{50}	T_{90}	
SPUA1	191.65	317.17	389.98	183.48
				291.34
				352.34
SPUA2	199.67	340.31	397.34	204.38
				308.34
				378.42
SPUA3	200.82	342.37	398.76	205.21
				320.41
				377.38
SPUA4	205.81	345.78	398.99	206.83
				329.36
				385.30
SPUA5	209.99	349.73	399.73	208.67
				339.36
				397.37

DMA analysis

DMA is a convenient and widely used method for examining the changes in the glass transition temperature (T_g) [12]. The loss factor ($\tan \delta$) of the films as a function of temperature for

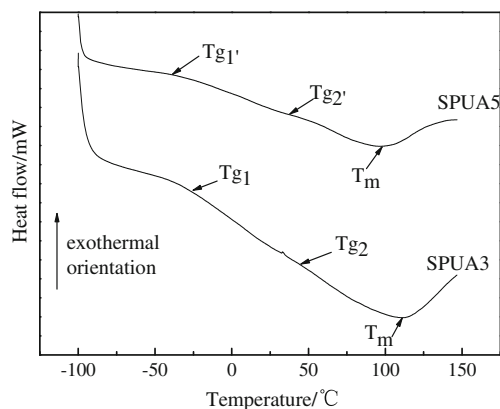


Fig. 8 DSC thermograms of SPUA3 and SPUA5 membranes

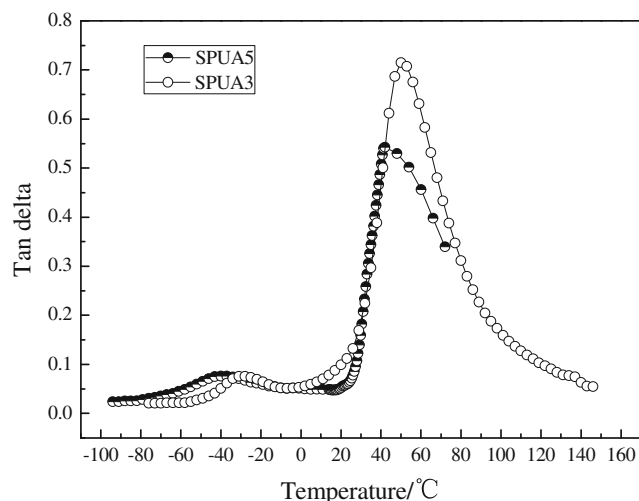


Fig. 9 The loss factor ($\tan\delta$) of the films as a function of temperature

the SPUA membranes with different SDNP content was shown in Fig. 9. The glass transition region was clearly performed as $\tan\delta$ peak in Fig. 9. It was shown that the specimens exist two $\tan\delta$ peaks corresponding to the DSC results (Fig. 8). The peak position of $\tan\delta$ for the SPUA3 and SPUA5 films, defined as T_g , are located at about -30.62°C , -40.18°C (soft segments) to 49.1°C , 42.51°C (hard segments). The T_g value decreased by increasing the SDNP content. The values are higher than that of the corresponding values determined by DSC as the measurements principle was different [12]. The height of $\tan\delta$ peak represents the homogeneity of the polymer film [28]. It was shown that the peak height reduced with the SDNP increased, suggesting that a more heterogeneous membranes was formed.

SEM analysis

The morphologies of the fractured surfaces of the SPUA1, SPUA3, and SPUA5 membranes were investigated by SEM as shown in Fig. 10. From Fig. 10, they all clearly demonstrated the coexistence of a dual phase. With the increment of the SDNP content, the miscibility of the hard and soft segment improved. The dual phase appears to be cocontinuous as well.

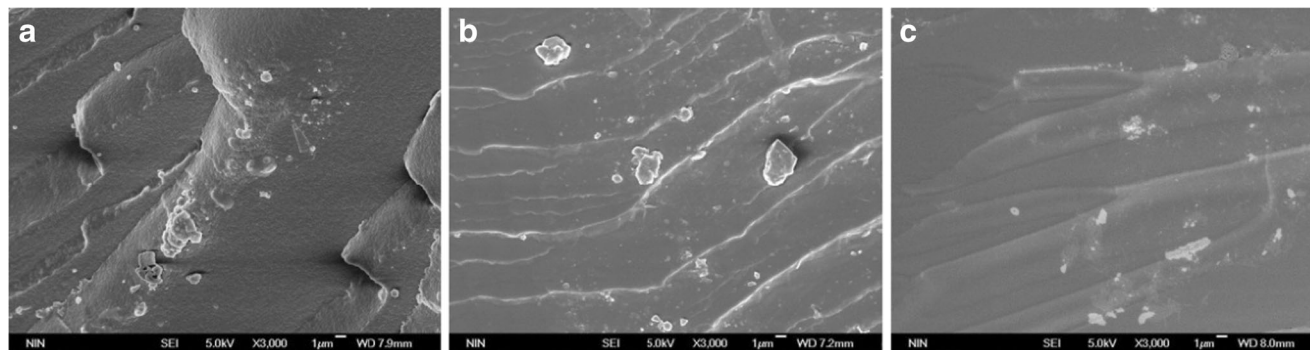


Fig. 10 SEM morphologies of SPUA1(a), SPUA3(b), SPUA5(c)

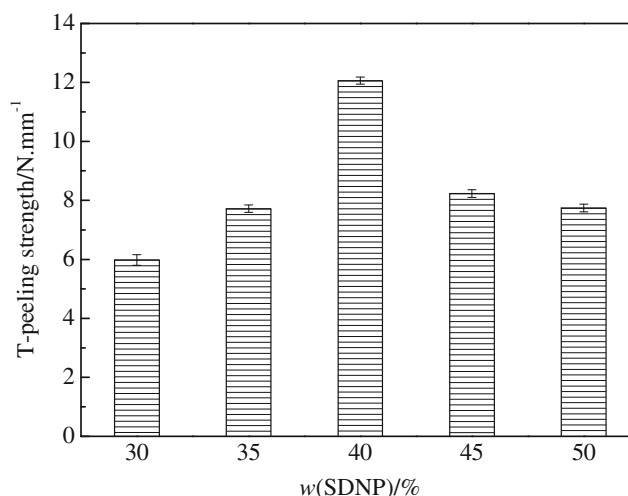


Fig. 11 The T-peel strength of the SPUA membranes as a function of the SDNP content

The microphase separation degree decreased significantly. As the addition of the sodium sulfonate groups in the soft segment, the density of the hydrogen bonding was increased, the interaction between the hard and soft domain was enhanced, so the microphase separation degree decreased. The results were in accordance with the TEM measurements. Meanwhile, with the addition of the PETA content, the crosslinking density was increased, which could make the hydrophobic polyacrylate easily diffuse into PU particles [29].

T-peel strength analysis

The adhesive properties of SPUA with different SDNP contents were measured, as shown in Fig. 11. The T-peel strength of the SPUA membranes increased from 5.98 N/mm to 12.06 N/mm when the SDNP content was up to 40 wt%. As the T-peel strength increased, an increase in adhesive strength is obtained [27]. With the increment of the sodium sulfonate groups with strong polar, the small particle size of the SPUA emulsion could penetrate into the substrates easily, and the particles could form hydrogen bonds with the polar groups of the substrates surface, therefore, the greater cohesive properties was formed. The increased interaction between the

Table 5 Surface tension, Contact angle, Interfacial tension of SPUA emulsions with different SDNP content

Samples	Surface tension (mN/m)	Contact angle(°)	Interfacial tension(mN/m)
SPUA1	46.1	43.2	4.44
SPUA2	46.53	43.8	4.47
SPUA3	46.92	44.4	4.53
SPUA4	47.02	44.6	4.57
SPUA5	47.89	45.7	4.60

SPUA and substrates surface were able to account for the enhanced adhesive strength. However, with the SDNP content increased higher than 40 wt%, the T-peel strength decreased to 7.74 N/mm. The increment of the SDNP content increased the miscibility of the hard and soft segments, which could restrain the sliding of the polymer chains. This phenomenon was detrimental to improve the adhesive, and this resulted in a decrease in the T-peel strength.

Wettability analysis

The wettability of SPUA emulsions on the substrates is very important for adhesion, while the surface tension is an important physical property parameter for the application performance of the SPUA emulsions. The surface tension of the SPUA emulsions and the contact angle of SPUA emulsion on the rubber surface were shown in Table 5. As seen in Table 5, the surface tension of the SPUA emulsions increased slightly with the increment of the SDNP content, and the contact angle of SPUA emulsions on the rubber surface also increased, which indicated that the wettability of SPUA emulsions on the rubber surface decreased. The wettability of SPUA emulsion on the rubber surface can be quantified by the interfacial tension: the lower the interfacial tension was, the better the wettability was [28]. Based on Young's eq. (1), the interfacial tension (γ_{SL}) can be calculated by the measured contact angles [30].

$$\gamma_S = \gamma_{SL} + \gamma_L \cos\theta \quad (1)$$

where θ is the contact angle of SPUA emulsions on the rubber surface, γ_S is the surface tension of the rubber surface (the value was 38.05 mN/m), γ_L is the surface tension of SPUA emulsions (measured in Table 5), respectively. The results of γ_{SL} are calculated and also listed in Table 5. From Table 5, it can be seen that with the increment of SDNP content, the value of γ_{SL} increased gradually, which demonstrated that the wettability of the SPUA emulsions on the rubber surface also decreased. Nevertheless, the increment degree of the surface tension, contact angle, and interfacial tension

was not so great, so the influence of the SDNP content on the wettability of SPUA emulsions on the rubber surface is not distinct. Moreover, the contact angle, ranged from 43.2° to 45.7°, was a relatively low value, which showed that the SPUA emulsions can wet the rubber surface well.

Conclusions

A series of sulfonated polyurethane/polyacrylate (SPUA) emulsions were successfully prepared by soap-free emulsion polymerization. Effect of sodium sulfonate modified polyester polyol (SDNP) on the properties of the emulsions and membranes were all studied. DLS result showed that with the increment of the SDNP content, the particle size first decreased and then increased. The TEM observation is consistent with the particle size results. ATR-FTIR result ascertains the formation of SPUA. XPS analysis demonstrates the SDNP were successfully reacted in preparation of the SPUA emulsions. With the increment of SDNP content, the SPUA membranes showed higher tensile strength and lower breaking elongation. TGA showed that the thermal stability of the SPUA membranes was enhanced by increasing the SDNP content. SEM results demonstrates that the miscibility of the hard and soft segment improved. The SPUA emulsions could be used as adhesives since the T-peel strength and wettability all displayed well.

Acknowledgements This project was supported by the Graduate Innovation Fund of Shaanxi University of Science & Technology, and the authors would also like to thank the National Natural Science Foundation of China (contract grant number: 51373091), the specialized research fund of Xianyang Normal University Project (14XSYK014) for financial support.

References

- Földes E, Tóth A, Kálmán E, Fekete E, Tomasoovszky-Bobák á (2000) Surface changes of corona-discharge-treated polyethylene films. *J Appl Polym Sci* 76(10):1529–1541.
- Kim BK, Shin JH (2002) Modification of waterborne polyurethane by forming latex interpenetrating polymer networks with acrylate rubber. *Colloid Polym Sci* 280(8):716–724
- Sundar S, Tharanikkarasu K, Dhathathreyan A, Radhakrishnan G (2002) Aqueous dispersions of poly(urethane-co-vinylpyridine) synthesised from polyurethane macroiniferter. *Colloid Polym Sci* 280(10):915–921
- Lewandowski K, Krepski LR, Mickus DE., Roberts RR, S. Heilmann M, Larson WK, Purgett MD, Koecher SD, Johnson SA, McGurran DJ, Rueb CJ, Pathre SV, Thakur KAM (2002) Synthesis and properties of waterborne self-crosslinkable sulfo-urethane silanol dispersions. *J Polym Sci, Polym Chem* 40(17):3037–3045.
- Lee HT, Wu SY, Jeng RJ (2006) Effects of sulfonated polyol on the properties of the resultant aqueous polyurethane dispersions. *Colloid Surf A* 276(1–3):176–185

6. Kim IH, Shin JS, Cheong IW, Kim JI, Kim JH (2002) Seeded emulsion polymerization of methyl methacrylate using aqueous polyurethane dispersion: effect of hard segment on grafting efficiency. *Colloid Surf A* 207(1–3):169–176
7. Wen TC, Tseng HS, Lu ZB (2000) Co-solvent effect on conductivity of composite electrolytes comprising polyethylene oxide and polytetramethylene glycol-based waterborne polyurethane via a mixture design approach. *Solid State Ionics* 134(3–4):291–301
8. Wang HL, Gopalan A, Wen TC (2003) A novel lithium single ion based polyurethane electrolyte for light-emitting electrochemical cell. *Mater Chem Phys* 82(3):793–800
9. Mequanint K, Sanderson R (2003) Nano-structure phosphorus-containing polyurethane dispersions: synthesis and crosslinking with melamine formaldehyde resin. *Polymer* 44(9):2631–2639
10. Nomula S, Cooper SL (2001) Ionomer solution structure and solution diagram. *Macromolecules* 34(8):2653–2659
11. Wang XR, Shen YD, Lai XJ (2014) Micromorphology and mechanism of polyurethane/polyacrylate membranes modified with epoxide group. *Prog Org Coat* 77(1):268–276
12. Wang XR, Shen YD, Lai XJ, Liu GJ, Du Y (2014) Micromorphology and thermal properties of polyurethane/polyacrylate soap-free emulsion in the presence of functional monomers. *J Polym Res* 21(3):367
13. Adler HJ, Jahny K, Vogt-Birnbrich B (2001) Polyurethane macromers-new building blocks for acrylic hybrid emulsions with outstanding performance. *Prog Org Coat* 43(4):251–257
14. Darwish MA, Machunsky S, Peuker U, Kunz U, Turek T (2011) Magnetite core-shell nano-composites with chlorine functionality: preparation by miniemulsion polymerization and characterization. *J Polym Res* 18(1):79–88
15. Xin H, Shen YD, Li XR (2011) Novel cationic polyurethane-fluorinated acrylic hybrid latexes: synthesis, characterization and properties. *Colloid Surf A* 384(1–3):205–211
16. Jang JY, Jhon YK, Cheong IW, Kim JH (2002) Effect of process variables on molecular weight and mechanical properties of water-based polyurethane dispersion. *Colloid Surf A* 196(2–3):135–143
17. Honarkar H, Barmar M, Barikani M (2016) New sulfonated waterborne polyurethane dispersions: preparation and characterization. *J Disper Sci Technol* 37(8):1219–1225
18. Athawale VD, Kulkarni MA (2010) Synthesis, characterization, and comparison of polyurethane dispersions based on highly versatile anionomer, ATBS, and conventional DMPA. *J Coating Technol Res* 7(2):189–199
19. Zhou XH, Tu WP, Hu JQ (2006) Preparation and characterization of two-component waterborne polyurethane comprised of water-soluble acrylic resin and HDI biuret. *Chinese J Chem Eng* 14(1):99–104
20. Xiao XY, Wang Y (2009) Emulsion copolymerization of fluorinated acrylate in the presence of a polymerizable emulsifier. *Colloid Surf A* 348(1–3):151–156
21. Sanchis MR, Calvo O, Fenollar O, Garcia D, Balart R (2008) Characterization of the surface changes and the aging effects of low-pressure nitrogen plasma treatment in a polyurethane film. *Polym Test* 27(1):75–83
22. Takahashi K, Nagai K (1996) Preparation of reactive polymeric microspheres by seeded copolymerization using a polymerizable surfactant bearing an active ester group. *Polymer* 37(7):1257–1266
23. Chattopadhyay DK, Sreedhar B, Raju K VSN (2005) Effect of chain extender on phase mixing and coating properties of polyurethane Ureas. *Ind Eng Chem Res* 44(6):1772–1779
24. Ramezanzadeh B, Ghasemi E, Mahdavian M, Changizi E, Mohammadzadeh Moghadam MH (2015) Characterization of covalently-grafted polyisocyanate chains onto graphene oxide for polyurethane composites with improved mechanical properties. *Chem Eng J* 281:869–883
25. Zhang SB, Jiang HM, Xu YM, Zhang DH (2007) Thermal and crystalline properties of water-borne polyurethanes based on IPDI, DMPA, and PEBA/HNA. *J Appl Polym Sci* 103(3):1936–1941
26. Coutinho FMB, Delpech MC, Alves TL, Ferreira AA (2003) Degradation profiles of cast films of polyurethane and poly(urethane-urea) aqueous dispersions based on hydroxy-terminated polybutadiene and different diisocyanates. *Polym Degrad Stab* 81(1):19–27
27. Pérez-Limiñana MA, Arán-Aís F, Torró-Palau AM, César Orgilés-Barceló A, Miguel Martín-Martínez J (2005) Characterization of waterborne polyurethane adhesives containing different amounts of ionic groups. *Int J Adhes Adhes* 25(6):507–517
28. Lei L, Xia ZB, Ou CB, Zhang L, Zhong L (2015) Effects of crosslinking on adhesion behavior of waterborne polyurethane ink binder. *Prog Org Coat* 88:155–163
29. Park DH, Oh JK, Kim SB, Kim WN (2013) Synthesis and characterization of sulfonated polyol-based waterborne polyurethane-polyacrylate hybrid emulsions. *Macromol Res* 21(11):1247–1253
30. Hu D, Li L, Li YX, Yang CF (2017) Restructuring the surface of polyurethane resin enforced filter media to separate surfactant stabilized oil-in-water emulsions via coalescence. *Sep Purif Technol* 172:59–67